AIMS Mathematics, 11(4): 8945–8965.
DOI: 10.3934/math.2026369
Received: 24 January 2026
Revised: 09 March 2026
Accepted: 18 March 2026
Published: 01 April 2026

https://www.aimspress.com/journal/Math

*Research article*

# A logarithmic–gamma frailty model for first-failure times with heavy-tailed risk

**Mohieddine Rahmouni***

Applied College, King Faisal University, Al-Ahsa, Saudi Arabia

* **Correspondence:** Email: mrahmouni@kfu.edu.sa.

**Abstract:** We propose a new lifetime distribution for first-failure times in heterogeneous systems by combining exponential component lifetimes with a shared gamma frailty and a logarithmic distribution governing the latent number of competing failure causes. The model is constructed as the minimum lifetime among a random number of conditionally exponential components, where the system size follows a logarithmic distribution, and all components share an unobserved gamma-distributed risk factor. The resulting marginal distribution is a logarithmic mixture of Lomax distributions and admits tractable series expressions for the probability density, distribution, survival, and hazard functions. We show that the conditional model $Y \mid N = n$ has a strictly decreasing failure rate and exhibits heavy-tailed behavior. We investigate the marginal hazard behavior of the proposed mixture numerically, and classical models such as the exponential–logarithmic, Lomax, and exponential distributions arise as limiting cases. Maximum likelihood and expectation–maximization (EM)-type estimation procedures are developed, and the flexibility of the model is illustrated through simulation and a real data application. In first-failure-only settings, the logarithmic mixing parameter $\eta$ may be weakly identifiable and therefore difficult to estimate reliably from the observed data alone.

**Keywords:** first-failure time; logarithmic distribution; gamma frailty; Lomax distribution; heavy tails
**Mathematics Subject Classification:** 60E05, 62E15, 62F10

## 1. Introduction

Modeling time-to-event data plays a central role in reliability engineering [1–3], biomedical survival analysis [4, 5], actuarial science [6–8], and finance [9, 10]. In many practical situations, the observed lifetime corresponds to the time until the *first-failure* among multiple latent failure-prone components [11, 12]. Such data often exhibit three prominent empirical features: (i) Decreasing failure rates, reflecting early failures or infant mortality effects [13]; (ii) heavy-tailed survival behavior, indicating the presence of extreme events [14]; and (iii) unobserved heterogeneity among experimental

units or systems [15].

Classical lifetime distributions, including the exponential and Weibull models, are attractive due to their mathematical simplicity, but they are often insufficient for capturing these features simultaneously. In particular, the exponential distribution imposes a constant hazard rate and cannot accommodate either heterogeneity or heavy tails, and the Weibull distribution requires careful tuning of its shape parameter and still lacks an explicit mechanism for latent variability [16, 17].

One influential line of research models first-failure times through systems with a random number of parallel components. A seminal example is the exponential–geometric (EG) distribution, which assumes exponentially distributed component lifetimes and a geometrically distributed system size [18]. This construction yields a decreasing failure rate and a simple mixture representation, making it popular in reliability and survival studies. Numerous extensions have since been proposed, including generalized geometric, truncated geometric, and power-series-based models.

A complementary and widely used approach to modeling lifetime heterogeneity is frailty modeling [19–21]. Frailty introduces an unobserved random effect that acts multiplicatively on the hazard function, capturing latent variability across individuals or systems. Among the available frailty distributions, the gamma distribution is particularly appealing due to its analytical tractability and interpretability. When applied to exponential lifetimes, gamma frailty induces the Lomax (Pareto type II) distribution, which exhibits heavy tails and a monotonically decreasing hazard rate [20, 22, 23].

Recent work has unified geometric redundancy models and gamma frailty in the first-failure setting, producing a flexible family of distributions that bridge the exponential–geometric and Lomax models through limiting arguments. These unified models combine random system size with shared frailty, yielding geometric mixtures of Lomax distributions with clear probabilistic interpretation and tractable inference [17].

Despite these advances, existing first-failure frailty models rely almost exclusively on geometric or Poisson mixing mechanisms for the system size. These distributions assign rapidly decaying probabilities to large system sizes and may therefore underrepresent scenarios involving extreme redundancy or clustering of latent failure causes. In many applied contexts, such as financial risk aggregation, cybersecurity incidents, epidemic outbreaks, or complex engineering systems, rare but severe clustering effects play a crucial role in shaping early-failure behavior and tail risk.

The logarithmic distribution provides a natural alternative for modeling such phenomena. Unlike geometric or Poisson distributions, the logarithmic distribution places relatively greater mass on larger counts and is well-suited to representing rare but severe aggregation mechanisms [24–26]. Despite its relevance, logarithmic mixing has received limited attention in first-failure frailty models, particularly in conjunction with gamma frailty and exponential baselines.

The objective of this paper is to address this gap by introducing a *logarithmic–gamma frailty model* for first-failure times. We consider a system composed of a random number of parallel components, where the system size follows a logarithmic distribution, and component lifetimes are conditionally exponential given a shared gamma frailty. The observed lifetime is defined as the time to the first component failure. The resulting marginal distribution is a logarithmic mixture of Lomax distributions with heavy-tailed behavior; moreover, conditional on $N = n$, the model reduces to a Lomax law with a strictly decreasing hazard rate, and the marginal hazard behavior of the mixture is examined numerically.

The proposed model generalizes several classical distributions as limiting cases, including

the exponential–logarithmic, Lomax, and exponential models. Moreover, it preserves analytical tractability while providing enhanced flexibility for modeling early failures and tail risk.

Throughout this paper, we focus on first-failure observations. Because first-failure data record only the minimum among latent component lifetimes, the mixing parameter $\eta$ can be weakly identifiable in practice; the logarithmic mixing mechanism may be more informative in settings where more than the minimum is observed, such as multiple-failure, repeated-event, or competing-risks designs.

The remainder of the paper is organized as follows. Section 2 derives the distribution of the first-failure time under the proposed hierarchical model. Section 3 investigates its distributional properties, including the shape of the density, survival and hazard functions, tail behavior, and limiting cases. Estimation procedures are given in Section 4. Simulation results are reported in Section 5. A real-data application is presented in Section 6, and Section 7 concludes.

## 2. Distribution derivation

We now introduce the hierarchical construction of the logarithmic–gamma frailty (LGF) model. Let $N$ denote the random number of latent failure-prone components in the system. For $\eta \in (0,1)$, we assume that $N$ follows a logarithmic distribution with probability mass function (PMF)

$$\Pr(N=n) = \frac{\eta^n}{-n\log(1-\eta)}, \quad n = 1,2,\ldots \tag{2.1}$$

To ensure the model is mathematically nested within a broader family of distributions, we adopt the continuous extension $\eta \in [0,1)$. Here, the boundary case $\eta = 0$ is interpreted as the pointwise limit of the PMF:

$$\lim_{\eta \downarrow 0} \Pr(N=n) = \begin{cases} 1, & n=1, \\ 0, & n \geq 2. \end{cases} \tag{2.2}$$

Consequently, at $\eta = 0$, the mixing mechanism collapses to a deterministic system size $N \equiv 1$, allowing the LGF model to reduce to the classical Lomax submodel.

To account for unobserved heterogeneity, let $Z$ denote a shared frailty variable following a gamma distribution with shape and rate parameters both equal to $\lambda > 0$:

$$Z \sim \Gamma(\lambda,\lambda), \quad \text{with } \mathbb{E}(Z) = 1 \text{ and } \mathrm{Var}(Z) = 1/\lambda. \tag{2.3}$$

Conditional on the realized frailty $Z = z$ and the realized number of components $N = n$, the individual component lifetimes $X_1,\ldots,X_n$ are assumed to be independent and identically distributed (i.i.d.) exponential random variables with rate $\theta z$:

$$X_i \mid (Z=z, N=n) \sim \mathrm{Exp}(\theta z), \quad i = 1,\ldots,n, \tag{2.4}$$

where $\theta > 0$ is the baseline scale parameter. Finally, the observed system lifetime is defined as the first-failure time, $Y = \min\{X_1,\ldots,X_N\}$. This hierarchical structure integrates three distinct sources of risk: The baseline failure intensity ($\theta$), unobserved heterogeneity ($\lambda$), and the shape of the random system size distribution ($\eta$).

*2.1. Conditional distribution given the system size*

Conditional on $N = n$ and $Z = z$, the minimum of $n$ independent exponential random variables with rate $\theta z$ is itself exponential with rate $n\theta z$. Hence, the conditional density of $Y$ given $N = n$ and $Z = z$ is

$$f_{Y|N=n,Z=z}(y) = n\theta z e^{-n\theta zy}, \quad y > 0. \tag{2.5}$$

To account for unobserved heterogeneity, we integrate out the frailty variable $Z$.

*2.2. Marginal distribution given the system size*

**Theorem 1.** *Let $Y$ denote the first-failure time under the proposed hierarchical model. Conditional on $N = n$, the marginal density of $Y$ is*

$$f_{Y|N=n}(y) = \frac{n\theta\lambda^{\lambda+1}}{(\lambda + n\theta y)^{\lambda+1}}, \quad y > 0. \tag{2.6}$$

*Proof.* We integrate the conditional density with respect to the gamma frailty:

$$f_{Y|N=n}(y) = \int_0^\infty n\theta z e^{-n\theta zy} \frac{\lambda^\lambda}{\Gamma(\lambda)} z^{\lambda-1} e^{-\lambda z} dz.$$

Rearranging terms yields

$$f_{Y|N=n}(y) = \frac{n\theta\lambda^\lambda}{\Gamma(\lambda)} \int_0^\infty z^\lambda e^{-(\lambda+n\theta y)z} dz.$$

Using the standard gamma integral

$$\int_0^\infty z^a e^{-bz} dz = \frac{\Gamma(a+1)}{b^{a+1}}, \quad a > -1,\ b > 0,$$

with $a = \lambda$ and $b = \lambda + n\theta y$, we obtain

$$f_{Y|N=n}(y) = \frac{n\theta\lambda^\lambda \Gamma(\lambda+1)}{\Gamma(\lambda)(\lambda + n\theta y)^{\lambda+1}} = \frac{n\theta\lambda^{\lambda+1}}{(\lambda + n\theta y)^{\lambda+1}}.$$

□

Thus, conditional on $N = n$, the first-failure time follows a Lomax distribution with shape parameter $\lambda$ and scale parameter $\lambda/(n\theta)$.

*2.3. Marginal distribution of the first-failure time*

We now average over the logarithmic distribution of $N$.

**Theorem 2.** *(Marginal PDF) The marginal probability density function of the first-failure time $Y$ is*

$$f_Y(y) = \frac{\theta\lambda^{\lambda+1}}{-\log(1-\eta)} \sum_{n=1}^\infty \frac{\eta^n}{(\lambda + n\theta y)^{\lambda+1}}, \quad y > 0. \tag{2.7}$$

*Proof.* The result follows by summing $f_{Y|N=n}(y)$ weighted by $\Pr(N = n)$ over $n \geq 1$. □

**Corollary 3.** *(Logarithmic mixture representation) The distribution of $Y$ is a logarithmic mixture of Lomax distributions:*

$$Y \sim \sum_{n=1}^\infty \frac{\eta^n}{-n\log(1-\eta)} \cdot \text{Lomax}\left(\lambda, \frac{\lambda}{n\theta}\right).$$

## 3. Distributional properties

This section investigates the main distributional features of the proposed logarithmic–gamma frailty model for first–failure times. We study the shape of the density, distribution and hazard behavior, tail properties and asymptotics, quantile behavior, limiting distributions, and stochastic ordering properties.

### *3.1. Shape of the density*

The PDF $f_Y(y)$ is expressed as a positive linear combination of Lomax densities with a common shape parameter $\lambda$ and scale parameters depending on the latent system size. Because each Lomax component is strictly decreasing, the mixture inherits this property.

**Proposition 4.** *$f_Y(y)$ is strictly decreasing on $(0,\infty)$ and attains its global maximum at $y = 0$.*

*Proof.* Each Lomax density appearing in the mixture representation of $f_Y(y)$ is strictly decreasing in $y$. Because the mixture weights are positive and sum to one, their weighted average is also strictly decreasing. □

Evaluating the density at the origin yields

$$f_Y(0) = \frac{\theta}{-\log(1-\eta)} \sum_{n=1}^{\infty} \frac{\eta^n}{n} = \frac{\theta}{-\log(1-\eta)},$$

where the last equality follows from the identity $\sum_{n=1}^{\infty} \eta^n/n = -\log(1-\eta)$ for $\eta \in [0,1)$.

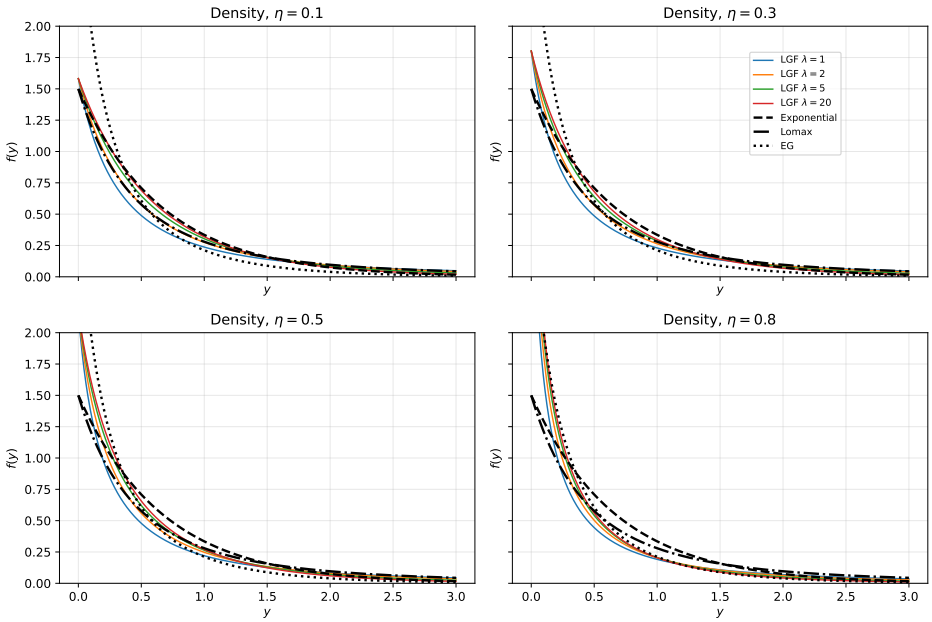


**Figure 1.** Density functions of the logarithmic–gamma frailty model for $\theta = 1.5$. Panels correspond to $\eta \in \{0.1,\ 0.3,\ 0.5,\ 0.8\}$. Within each panel, unified LGF densities for $\lambda \in \{1,\ 2,\ 5,\ 20\}$ are compared with the exponential, Lomax, and exponential–geometric (EG) densities. Increasing $\eta$ shifts mass toward the origin, whereas larger values of $\lambda$ produce lighter tails.

Figure 1 illustrates the flexibility of the proposed model. The logarithmic parameter $\eta$ primarily controls early-failure behavior, and the frailty parameter $\lambda$ governs tail thickness.

### 3.2. Distribution, survival, and hazard functions

The cumulative distribution function of $Y$ is given by

$$F_Y(y) = 1 - \frac{1}{-\log(1-\eta)} \sum_{n=1}^{\infty} \frac{\eta^n}{n} \left( \frac{\lambda}{\lambda + n\theta y} \right)^{\lambda}, \tag{3.1}$$

and the corresponding survival function is

$$S_Y(y) = \frac{1}{-\log(1-\eta)} \sum_{n=1}^{\infty} \frac{\eta^n}{n} \left( \frac{\lambda}{\lambda + n\theta y} \right)^{\lambda}. \tag{3.2}$$

The hazard rate function is defined as

$$h_Y(y) = \frac{f_Y(y)}{S_Y(y)}.$$

Although each component $Y \mid N = n$ has a decreasing hazard rate, monotone hazard properties are not automatically preserved under mixing, because the marginal hazard $h_Y(y) = f_Y(y)/S_Y(y)$ depends on $y$-varying posterior weights over $n$. Therefore, we do not state a general decreasing-failure-rate (DFR) theorem for the marginal LGF model, and instead examine the marginal hazard shape numerically for representative parameter settings.

**Proposition 5.** *For any fixed integer $n \geq 1$, the conditional hazard rate $h(y \mid N = n)$ is strictly decreasing for $y > 0$.*

*Proof.* By Theorem 1, $Y \mid N = n$ follows a Lomax distribution with shape parameter $\lambda$ and scale parameter $\lambda/(n\theta)$. The Lomax hazard rate is strictly decreasing for $y > 0$, and, $h(y \mid N = n)$ is strictly decreasing. □

We emphasize that this conditional monotonicity does not, in general, imply that the marginal hazard rate $h_Y(y) = f_Y(y)/S_Y(y)$ of the logarithmic mixture is globally decreasing, because mixture hazards involve $y$-dependent posterior weights.

Figure 2 illustrates typical marginal hazard shapes of the proposed model across parameter settings and highlights the role of logarithmic mixing relative to classical competitors.

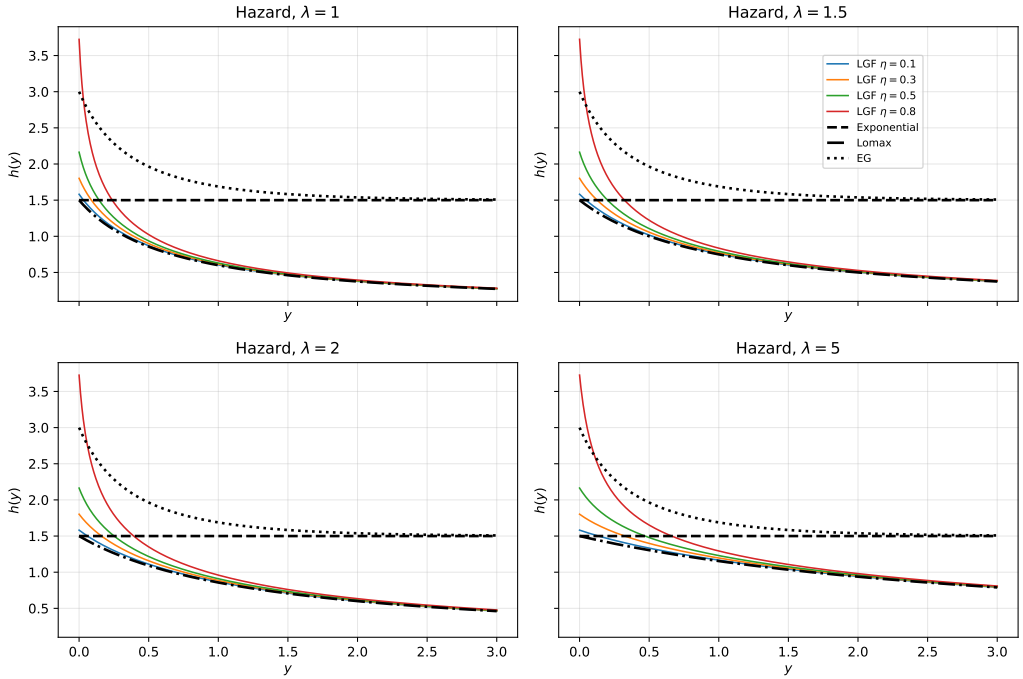


**Figure 2.** Hazard functions of the logarithmic–gamma frailty model for $\theta = 1.5$. Panels correspond to $\lambda \in \{1,\ 1.5,\ 2,\ 5\}$. Within each panel, unified LGF curves vary over $\eta \in \{0.1,\ 0.3,\ 0.5,\ 0.8\}$ and are compared with the exponential, Lomax, and EG hazard functions. Increasing $\eta$ strengthens early-failure concentration, whereas larger values of $\lambda$ reduce heterogeneity.

### *3.3. Tail behavior and limiting distributions*

As $y \to \infty$, the survival function exhibits regularly varying behavior, satisfying

$$S_Y(y) \sim C(\eta,\lambda)\, y^{-\lambda}, \qquad h_Y(y) \sim \frac{\lambda}{y},$$

where $C(\eta,\ \lambda) > 0$ is a finite constant depending on the logarithmic mixing mechanism. Consequently, the tail index of the distribution is governed entirely by the frailty parameter $\lambda$.

Several classical lifetime distributions arise as limiting cases of the proposed model.

**Theorem 6.** *On the extended parameter space $\eta \in [0,1)$, the boundary case $\eta = 0$ corresponds to the Lomax submodel, and as $\eta \downarrow 0$, the survival function $S_Y(y;\ \eta)$ converges pointwise to the Lomax survival function*

$$\left(\frac{\lambda}{\lambda+\theta y}\right)^{\lambda}, \qquad y > 0,$$

*which implies convergence in distribution to the Lomax distribution with parameters $(\lambda,\theta)$.*

**Theorem 7.** *As $\lambda \to \infty$, the logarithmic–gamma frailty distribution converges to the exponential–logarithmic distribution.*

**Corollary 8.** *As $\eta \to 0$, and $\lambda \to \infty$, the model reduces to the exponential distribution with rate $\theta$.*

*3.4. Quantile function and stochastic ordering*

This subsection examines comparative properties of the proposed model through its quantile function and stochastic ordering. These results clarify how the logarithmic parameter $\eta$ influences the overall risk profile and enable formal comparisons between different parameter configurations.

**Quantile characterization.** Let $Q(p)$ denote the $p$th quantile of $Y$, defined implicitly by

$$S_Y(Q(p)) = 1 - p.$$

Although no closed-form expression is available, the quantile function satisfies

$$\sum_{n=1}^{\infty} \frac{\eta^n}{n} \left( \frac{\lambda}{\lambda + n\theta Q(p)} \right)^{\lambda} = (1-p)\,[-\log(1-\eta)], \tag{3.3}$$

which can be solved numerically using monotone root-finding algorithms.

**Asymptotic quantiles.** The regularly varying tail behavior established in Section 3.3 implies a simple approximation for extreme quantiles.

**Proposition 9.** *As $p \to 1$, the upper quantile satisfies*

$$Q(p) \sim \left( \frac{C(\eta, \lambda)}{1-p} \right)^{1/\lambda},$$

*where $C(\eta,\ \lambda)$ is the tail constant appearing in the asymptotic representation of the survival function.*

**Stochastic ordering.** The logarithmic parameter $\eta$ induces a natural stochastic ordering on the family of first-failure distributions.

**Proposition 10.** *Let $Y(\eta)$ denote the first-failure time with logarithmic parameter $\eta$. If $0 \le \eta_1 < \eta_2 < 1$, then*

$$Y(\eta_2) \le_{\text{st}} Y(\eta_1),$$

*that is, $Y(\eta_2)$ is stochastically smaller than $Y(\eta_1)$.*

*Proof.* To prove the stochastic ordering, it suffices to show that for each fixed $y > 0$, the survival function $S_Y(y;\ \eta)$ is decreasing in $\eta$. Write

$$S_Y(y;\eta) = \mathbb{E}_\eta[g(N)], \qquad g(n) = \left( \frac{\lambda}{\lambda + n\theta y} \right)^{\lambda},$$

where $g(n)$ is strictly decreasing in $n$ for each fixed $y > 0$. Because the logarithmic distribution of $N$ is stochastically increasing in $\eta$ (equivalently, it has a monotone likelihood ratio in $n$ in the parameter $\eta$), it follows that $\mathbb{E}_\eta[g(N)]$ is decreasing in $\eta$, and therefore, $S_Y(y;\ \eta)$ decreases in $\eta$ for all $y > 0$. Hence, $Y(\eta_2) \le_{\text{st}} Y(\eta_1)$ whenever $0 \le \eta_1 < \eta_2 < 1$. □

## 4. Statistical inference

This section develops likelihood-based inference for the proposed logarithmic–gamma frailty (LGF) model. We derive the observed-data likelihood, introduce a latent-variable representation that facilitates computation, and present estimation procedures based on direct maximization and the expectation–maximization (EM) algorithm. Numerical implementation details are also discussed.

### *4.1. Observed-data likelihood*

Let $y_1, \ldots, y_m$ denote an independent sample of first-failure times drawn from the LGF distribution with parameter vector $\psi = (\theta,\ \lambda,\ \eta)^\top$. From Section 3, the marginal density of $Y$ is

$$f_Y(y;\psi) = \frac{\theta\lambda^{\lambda+1}}{-\log(1-\eta)} \sum_{n=1}^{\infty} \frac{\eta^n}{(\lambda + n\theta y)^{\lambda+1}}, \qquad y > 0.$$

The observed-data log-likelihood is therefore

$$\ell(\psi) = m\log\theta + (\lambda+1)m\log\lambda - m\log[-\log(1-\eta)] + \sum_{i=1}^{m} \log\left( \sum_{n=1}^{\infty} \frac{\eta^n}{(\lambda + n\theta y_i)^{\lambda+1}} \right). \tag{4.1}$$

Direct maximization of $\ell(\psi)$ is possible using numerical optimization with truncated series approximations, but this approach can be computationally demanding. To address this issue, we exploit the latent structure of the model.

### *4.2. Latent-variable representation*

Recall that the LGF model admits the hierarchical representation

$$N \sim \text{Logarithmic}(\eta), \qquad Z \sim \Gamma(\lambda,\lambda), \qquad Y = \min\{X_1, \ldots, X_N\},$$

where, conditional on $Z = z$, the component lifetimes are independent $\text{Exp}(\theta z)$ variables.

Let $N_i$ and $Z_i$ denote the latent variables associated with observation $y_i$. The complete-data likelihood is then

$$L_c(\psi) = \prod_{i=1}^{m} \Pr(N_i = n_i) f_Z(z_i) f_{Y|N,Z}(y_i \mid n_i, z_i) \tag{4.2}$$

$$\propto \prod_{i=1}^{m} \frac{\eta^{n_i}}{n_i} \lambda^{\lambda} z_i^{\lambda-1} e^{-\lambda z_i} (n_i\theta z_i) e^{-n_i\theta z_i y_i}. \tag{4.3}$$

Taking logarithms yields the complete-data log-likelihood

$$\ell_c(\psi) = \sum_{i=1}^{m} \Big[ n_i\log\eta - \log n_i + \lambda\log\lambda + (\lambda-1)\log z_i - \lambda z_i + \log(n_i\theta z_i) - n_i\theta z_i y_i \Big] + \text{const.} \tag{4.4}$$

*4.3. EM algorithm*

To facilitate likelihood-based inference, we develop an EM algorithm by treating the latent system sizes $N_i$ and frailty variables $Z_i$ as missing data. This framework leverages the hierarchical structure of the model to simplify the maximization of the marginal likelihood.

**Complete-data formulation.** Let $(y_i,\ N_i,\ Z_i)$ denote the complete data associated with observation $i$, for $i = 1,\dots,m$. Up to an additive constant, the complete-data log-likelihood can be written as

$$\ell_c(\psi) = \sum_{i=1}^{m} \Big[ N_i \log \eta - \log N_i + \log \theta + (\lambda+1)\log \lambda \\ + (\lambda-1)\log Z_i - \lambda Z_i + \log(N_i Z_i) - N_i \theta Z_i y_i \Big], \tag{4.5}$$

where $\psi = (\theta,\ \lambda,\ \eta)^\top$.

**E-step.** At iteration $t$, the conditional distribution of $N_i$ given $y_i$ is

$$\Pr\big(N_i = n \mid y_i, \psi^{(t)}\big) = \frac{\eta^{(t)n}\big(\lambda^{(t)} + n\theta^{(t)} y_i\big)^{-(\lambda^{(t)}+1)}}{\sum_{k=1}^{\infty} \eta^{(t)k}\big(\lambda^{(t)} + k\theta^{(t)} y_i\big)^{-(\lambda^{(t)}+1)}}, \qquad n = 1,2,\dots, \tag{4.6}$$

where the factor $1/n$ from the logarithmic pmf cancels with the factor $n$ from the conditional exponential minimum density $f_{Y|N=n,Z=z}(y) = n\theta z e^{-n\theta z y}$.

Conditional on $(N_i = n,\ y_i)$ (and under $\psi^{(t)}$), the frailty variable satisfies

$$Z_i \mid (N_i = n, y_i) \sim \Gamma\Big(\lambda^{(t)} + 1,\ \lambda^{(t)} + n\theta^{(t)} y_i\Big) \tag{4.7}$$

so that

$$\mathbb{E}(Z_i \mid N_i = n, y_i) = \frac{\lambda^{(t)}+1}{\lambda^{(t)} + n\theta^{(t)} y_i}, \qquad \mathbb{E}(\log Z_i \mid N_i = n, y_i) = \psi\Big(\lambda^{(t)}+1\Big) - \log\Big(\lambda^{(t)} + n\theta^{(t)} y_i\Big),$$

with $\psi(\cdot)$ the digamma function.

The E-step therefore requires evaluation of

$$\mathbb{E}(N_i \mid y_i), \qquad \mathbb{E}(\log N_i \mid y_i), \qquad \mathbb{E}(N_i Z_i \mid y_i), \qquad \mathbb{E}(\log Z_i \mid y_i),$$

where expectations with respect to $N_i \mid y_i$ are computed using the posterior weights in (4.6).

In practice, all infinite sums are truncated adaptively at a level $K$ chosen so that the residual posterior mass $\sum_{k>K} \Pr(N_i = k \mid y_i)$ is below a fixed tolerance (e.g., $10^{-8}$), and the same tolerance is used consistently at each EM iteration.

**M-step.** The M-step maximizes the EM auxiliary function $Q(\psi \mid \psi^{(t)}) = \mathbb{E}\{\ell_c(\psi) \mid \mathbf{y}, \psi^{(t)}\}$ with respect to $\psi$.

***Implementation details (M-step).*** During each M-step, $\theta$ and $\lambda$ are updated by numerically maximizing $Q(\psi \mid \psi^{(t)})$ subject to $\theta > 0$ and $\lambda > 0$. We use a bound-constrained quasi-Newton routine (e.g., the limited-memory Broyden–Fletcher–Goldfarb–Shanno algorithm with box constraints (L-BFGS-B)), with convergence declared when the maximum absolute change in $(\theta,\ \lambda,\ \eta)$ is below $10^{-8}$ (or equivalently, when the increase in the observed-data log-likelihood is below $10^{-10}$). To reduce sensitivity to local optima, the EM algorithm is initialized from multiple dispersed starting values, and we retain the run that achieves the largest attained observed-data log-likelihood.

The update for $\eta$ is obtained by one-dimensional numerical maximization over $\eta \in [0,1)$.

$$\eta^{(t+1)} = \arg\max_{\eta\in[0,1)} Q\big(\eta \mid \psi^{(t)}\big). \tag{4.8}$$

Equivalently, $\eta^{(t+1)}$ solves the score equation

$$\frac{\partial}{\partial\eta} Q\big(\eta \mid \psi^{(t)}\big) = \frac{\sum_{i=1}^{m} \mathbb{E}(N_i \mid y_i)}{\eta} - \frac{m}{(1-\eta)\,[-\log(1-\eta)]} = 0, \qquad \eta \in (0,1), \tag{4.9}$$

which is solved numerically using a safeguarded Newton or bisection routine on $\eta \in [0,1)$ with a tolerance of $10^{-8}$.

The parameters $\theta$ and $\lambda$ do not admit closed-form updates in the general three-parameter case and are obtained by numerical maximization of $Q(\psi \mid \psi^{(t)})$ (or equivalently by solving the corresponding score equations via Newton–Raphson and/or quasi-Newton methods).

Although the EM framework applies formally to all parameters, weak identifiability can make EM-based joint estimation of $(\theta,\ \lambda,\ \eta)$ numerically unstable in finite samples; therefore, in the simulation study, we fix $\lambda$ to focus on the estimability of $(\theta,\ \eta)$, whereas the real-data application reports full maximum likelihood estimates obtained by direct maximization of the observed-data log-likelihood.

**Validation of EM instability under joint estimation.** To substantiate the instability of EM-based joint estimation of $(\theta,\ \lambda,\ \eta)$ under first-failure data, we performed multiple-start experiments and likelihood diagnostics. When updating all three parameters by EM, we observed sensitivity to initialization and frequent convergence to boundary or local solutions (notably for $\eta$), consistent with weak curvature in the $\eta$ direction. This behavior motivates fixing $\lambda$ in the simulation study to isolate inference for $(\theta,\ \eta)$. In contrast, in the real-data application we estimate all parameters by direct maximization with multiple starting values and verify convergence to the same maximized log-likelihood within numerical tolerance.

### *4.4. Direct numerical maximization*

As an alternative to EM, the model parameters can be estimated by direct maximization of the observed-data log-likelihood. In practice, the infinite sums appearing in the likelihood (and its derivatives) are approximated by truncation at a finite level $K$, chosen so that the residual mass is below a fixed tolerance. The appendix (Robustness analysis) demonstrates that the resulting parameter estimates are insensitive to $K$ beyond moderate truncation levels.

*4.5. EM versus direct numerical maximization (comparative assessment)*

We compared EM with direct maximization of the observed-data log-likelihood using the same truncation tolerance (e.g., $10^{-8}$). When both methods converged to the same optimum, the resulting parameter estimates and maximized log–likelihood values agreed up to numerical precision. In settings exhibiting weak identifiability in $\eta$, EM was more sensitive to initialization, and direct maximization with multiple starting values provided a convenient stability check via repeated convergence to the same maximized log-likelihood.

## 5. Simulation study

This section investigates the finite-sample behavior of likelihood-based estimation for the proposed logarithmic–gamma frailty (LGF) model via a Monte Carlo study. The primary objective is to assess the estimability of the baseline scale parameter $\theta$ and the logarithmic mixing parameter $\eta$ from first-failure data. To focus on the behavior of $(\theta,\ \eta)$ under first-failure sampling, the frailty shape parameter $\lambda$ is treated as known and fixed at its data-generating value throughout this section.

Fixing $\lambda$ is motivated both practically and methodologically. In some applications, $\lambda$ may be informed by external reliability studies, historical datasets, or domain-based calibration of heterogeneity. From an inferential standpoint, holding $\lambda$ fixed isolates the intrinsic identifiability of the logarithmic mixing mechanism from numerical issues in three-parameter estimation. As demonstrated below, even under this favorable configuration, estimation of $\eta$ can remain challenging due to weak identifiability under first-failure sampling; we further diagnose this behavior using profile log-likelihoods in $\eta$.

*Data generation and simulation scenarios*

Data are generated according to the hierarchical LGF model described in Section 2. For each observation $i = 1,\ldots,n$:

1. The latent system size is drawn as $N_i \sim \text{Logarithmic}(\eta)$.
2. A shared frailty variable is generated as $Z_i \sim \Gamma(\lambda,\lambda)$, ensuring $\mathbb{E}(Z_i) = 1$.
3. Conditional on $(N_i, Z_i)$, component lifetimes are independent and exponentially distributed with rate $\theta Z_i$.
4. The observed lifetime is the first-failure time $Y_i = \min\{X_{i1},\ldots,X_{iN_i}\}$.

Four scenarios are considered to represent a broad range of tail behavior and mixing intensity:

- **Baseline:** $(\theta,\ \lambda,\ \eta) = (1.0,\ 5.0,\ 0.30)$, representing moderate frailty variance and moderate logarithmic mixing.
- **Lomax-like:** $(1.0,\ 5.0,\ 0.01)$, corresponding to extremely small mixing and pronounced early failures.
- **High-variance:** $(1.0,\ 1.5,\ 0.50)$, characterized by substantial unobserved heterogeneity.
- **EG-like:** $(1.0,\ 20.0,\ 0.40)$, where frailty variance is small and the model approaches an exponential–geometric regime.

For each scenario, sample sizes $n \in \{50,\ 100,\ 200,\ 500,\ 800\}$ are examined, and $R = 200$ independent replications are generated.

*Estimation via a fast EM algorithm*

Parameter estimation is carried out using a fast EM algorithm with $\lambda$ fixed at its true value. In the E-step, posterior weights

$$w_{ik} = P(N_i = k \mid y_i) \propto \frac{\eta^k}{(\lambda + k\theta y_i)^{\lambda+1}}, \qquad k = 1, \ldots, K,$$

are computed using a truncated representation with $K = 300$. This truncation level was verified empirically to yield negligible residual mass across all scenarios.

The parameter $\theta$ admits a closed-form update, whereas $\eta$ is updated by one-dimensional numerical maximization on $\eta \in [0, 1)$, consistent with Section 4:

$$\hat{\theta} = \frac{m}{\sum_{i=1}^{m} \mathbb{E}(N_i Z_i \mid y_i)\, y_i}, \qquad \hat{\eta} = \arg\max_{\eta \in [0,1)} Q\big(\eta \mid \psi^{(t)}\big).$$

In practice, the $\eta$ maximization is performed by a safeguarded Newton/bisection routine with a tolerance of $10^{-8}$.

*Simulation results*

Table 1 reports the empirical bias and root mean squared error (RMSE) of the estimators computed after implementing the corrected complete-data log-likelihood and the revised $\eta$ update described in Section 4.

The estimator $\hat{\theta}$ exhibits excellent finite-sample performance across all simulated scenarios. The bias remains negligible, and the RMSE decreases monotonically with increasing sample size $n$, closely adhering to the theoretical $n^{-1/2}$ rate* expected from the asymptotic normality of maximum likelihood estimators. For instance, in the high-variance scenario, a 16-fold increase in sample size (from $n = 50$ to $n = 800$) resulted in a nearly four-fold reduction in RMSE, which decreased from 0.367 to 0.125. Furthermore, the EM iterations proved to be numerically stable across all settings, with parameter updates successfully reaching the convergence criterion in the vast majority of replications.

In contrast, estimation of the logarithmic mixing parameter $\eta$ is substantially more challenging. Across scenarios, $\hat{\eta}$ can exhibit persistent bias whose magnitude decreases only slowly with increasing sample size under first-failure sampling. This effect is most pronounced in the Lomax-like configuration ($\eta = 0.01$), where $\hat{\eta}$ shows large positive bias across all sample sizes (e.g., bias $\approx 0.241$ at $n = 50$, and bias $\approx 0.179$ at $n = 800$), indicating slow improvement with increasing $n$. In other scenarios, the bias of $\hat{\eta}$ is smaller in magnitude and may be positive or negative, but can remain non-negligible in finite samples.

*The $n^{-1/2}$ (or $1/\sqrt{n}$) rate is the standard asymptotic convergence rate for maximum likelihood estimators under regularity conditions, where the variance of the estimator is inversely proportional to the sample size.

**Table 1.** Monte Carlo simulation results for the logarithmic–gamma frailty model with fixed frailty shape parameter ($\lambda$). Estimates of $\theta$ and $\eta$ are based on 200 replications. RMSE decreases with sample size for $\theta$, and $\eta$ exhibits persistent bias when near boundary values (e.g., Lomax-like scenario).

**(a)** Baseline ($\eta = 0.3$)

| $n$ | Param | True | Bias | RMSE |
|---|---|---|---|---|
| 50 | $\theta$ | 1.000 | -0.033 | 0.253 |
| | $\eta$ | 0.300 | 0.032 | 0.307 |
| 100 | $\theta$ | 1.000 | -0.038 | 0.195 |
| | $\eta$ | 0.300 | 0.064 | 0.279 |
| 200 | $\theta$ | 1.000 | -0.030 | 0.135 |
| | $\eta$ | 0.300 | 0.024 | 0.221 |
| 500 | $\theta$ | 1.000 | -0.029 | 0.105 |
| | $\eta$ | 0.300 | 0.039 | 0.186 |
| 800 | $\theta$ | 1.000 | -0.019 | 0.079 |
| | $\eta$ | 0.300 | 0.033 | 0.147 |

**(b)** Lomax-like ($\eta = 0.01$)

| $n$ | Param | True | Bias | RMSE |
|---|---|---|---|---|
| 50 | $\theta$ | 1.000 | -0.091 | 0.234 |
| | $\eta$ | 0.010 | 0.241 | 0.370 |
| 100 | $\theta$ | 1.000 | -0.084 | 0.178 |
| | $\eta$ | 0.010 | 0.245 | 0.352 |
| 200 | $\theta$ | 1.000 | -0.069 | 0.125 |
| | $\eta$ | 0.010 | 0.186 | 0.266 |
| 500 | $\theta$ | 1.000 | -0.067 | 0.102 |
| | $\eta$ | 0.010 | 0.191 | 0.249 |
| 800 | $\theta$ | 1.000 | -0.058 | 0.082 |
| | $\eta$ | 0.010 | 0.179 | 0.216 |

**(c)** High-variance ($\eta = 0.5$)

| $n$ | Param | True | Bias | RMSE |
|---|---|---|---|---|
| 50 | $\theta$ | 1.000 | 0.017 | 0.367 |
| | $\eta$ | 0.500 | -0.087 | 0.344 |
| 100 | $\theta$ | 1.000 | -0.000 | 0.289 |
| | $\eta$ | 0.500 | -0.039 | 0.305 |
| 200 | $\theta$ | 1.000 | -0.014 | 0.214 |
| | $\eta$ | 0.500 | -0.033 | 0.244 |
| 500 | $\theta$ | 1.000 | -0.016 | 0.147 |
| | $\eta$ | 0.500 | -0.003 | 0.175 |
| 800 | $\theta$ | 1.000 | -0.012 | 0.125 |
| | $\eta$ | 0.500 | 0.002 | 0.156 |

**(d)** EG-like ($\eta = 0.4$)

| $n$ | Param | True | Bias | RMSE |
|---|---|---|---|---|
| 50 | $\theta$ | 1.000 | -0.011 | 0.232 |
| | $\eta$ | 0.400 | -0.029 | 0.310 |
| 100 | $\theta$ | 1.000 | -0.007 | 0.167 |
| | $\eta$ | 0.400 | -0.010 | 0.258 |
| 200 | $\theta$ | 1.000 | 0.003 | 0.126 |
| | $\eta$ | 0.400 | -0.041 | 0.216 |
| 500 | $\theta$ | 1.000 | -0.009 | 0.092 |
| | $\eta$ | 0.400 | -0.005 | 0.170 |
| 800 | $\theta$ | 1.000 | 0.004 | 0.073 |
| | $\eta$ | 0.400 | -0.012 | 0.124 |

*Theoretical explanation: practical nonidentifiability of* $\eta$

The simulation patterns in Section 5 can be understood from the structure of the marginal likelihood. As shown in Eq (2.7), the observed density is a logarithmic mixture over the latent system size $N$. For a fixed observation $y$, terms associated with large $n$ are strongly down-weighted, so the likelihood is driven mainly by small values of $N$.

The mixing parameter $\eta$ governs the upper tail of the logarithmic distribution. In particular,

$$\Pr(N \geq k) = \frac{1}{-\log(1-\eta)} \sum_{n=k}^{\infty} \frac{\eta^n}{n}, \qquad k \geq 1,$$

so changes in $\eta$ primarily affect probabilities of large system sizes. Because first-failure data are comparatively insensitive to large-$N$ events, the log-likelihood can have weak curvature in the $\eta$ direction, leading to slow improvement of $\hat{\eta}$ with increasing sample size and, in some settings, noticeable finite-sample bias.

To diagnose this behavior, we examined the profile log-likelihood for $\eta$,

$$\ell_p(\eta) = \max_{\theta,\lambda} \ell(\theta, \lambda, \eta), \qquad \text{or (when } \lambda \text{ is fixed) } \ell_p(\eta) = \max_{\theta} \ell(\theta, \lambda_0, \eta).$$

Across the considered scenarios, $\ell_p(\eta)$ is often relatively flat over a broad range of $\eta$, corroborating that $\eta$ can be only weakly identified from first-failure data.

*Discussion and implications*

The simulation study reveals a clear separation in the inferential behavior of the LGF model parameters. The baseline scale parameter $\theta$ is well-identified and can be estimated reliably across all scenarios and sample sizes. By contrast, the logarithmic mixing parameter $\eta$ is only weakly identifiable from first-failure data and should be interpreted as a latent structural index rather than a consistently estimable quantity. Reliable inference for $\eta$ typically requires additional information beyond first-failure times, such as repeated or multiple failures per unit, partial or exact knowledge of system size, richer inspection or interval-censoring schemes that reveal more than the minimum, competing-risks information, or informative priors in a Bayesian formulation. In such settings, the logarithmic mixing mechanism can leave a clearer footprint in the data, and $\eta$ may become practically identifiable. Exploration of Bayesian/regularized approaches and designs with richer information is left for future research.

## 6. Real data application

We illustrate the proposed logarithmic–gamma frailty (LGF) model using the bladder cancer remission time dataset reported in [27]. The sample contains $n = 115$ remission times (in months), ranging from 0.08 to 79.05. This dataset is frequently used as a benchmark for lifetime models exhibiting substantial variability and potential heavy-tail behavior.

In this application, all model parameters are estimated by direct maximization of the observed-data log-likelihood (not by EM), using the L-BFGS-B algorithm with a convergence tolerance of $10^{-8}$ and a maximum of 2000 iterations. For the LGF likelihood, the infinite series is truncated at a sufficiently large level $K$ (here, $K = 3000$), and multiple dispersed starting values are employed; the reported solution corresponds to the largest attained log-likelihood, and repeated starts converge to the same maximized value within numerical tolerance.

For comparison, we fit the following models:

- Exponential (Exp.),

- Lomax,
- exponential–geometric (EG),
- logarithmic–gamma frailty (LGF).

Model adequacy is compared using the Aikake information criterion (AIC), the Bayesian information criterion (BIC), the Hannan–Quinn information criterion (HQIC), and the consistent Aikake information criterion (CAIC). These criteria are defined as below, respectively.

$$\mathrm{AIC} = -2\ell(\hat{\theta}) + 2q, \quad \mathrm{BIC} = -2\ell(\hat{\theta}) + q\log n,$$

$$\mathrm{HQIC} = -2\ell(\hat{\theta}) + 2q\log\log n, \quad \mathrm{CAIC} = -2\ell(\hat{\theta}) + q\frac{n\log n}{n-q-1},$$

where $\ell(\hat{\theta})$ is the maximized log-likelihood, $q$ is the number of parameters, and $n = 115$.

Table 2 shows that the exponential model attains the smallest values across all reported information criteria (e.g., AIC = 749.95), followed closely by the Lomax model (AIC = 750.52). The LGF fit yields $\hat{\eta} = 0.0000$, that is, the mixing parameter is estimated at the boundary of the extended parameter space $\eta \in [0,1)$. Consequently, the LGF likelihood collapses to its Lomax submodel and achieves essentially the same maximized log-likelihood as the Lomax fit ($-\log L = 373.26$), with nearly identical estimates $\hat{\theta} = 0.1161$ and $\hat{\lambda} \approx 10.82$. Because $\hat{\eta} = 0$ is a boundary estimate ($\eta \in [0,1)$), we do not report Wald standard errors for $\eta$.

Overall, these results indicate that, for this dataset, the likelihood provides no empirical support for $\eta > 0$ and the additional logarithmic mixing component does not improve fit beyond the nested Lomax alternative. In particular, because the LGF model incurs an additional parameter without increasing the maximized log-likelihood relative to Lomax, information criteria penalize LGF more strongly than Lomax.

**Table 2.** Parameter estimates and information criteria for the bladder cancer remission time data.

| Distribution | $\theta$ | $\lambda$ | $\eta$ | $-\log L$ | AIC | BIC | HQIC | CAIC |
|---|---|---|---|---|---|---|---|---|
| LGF | 0.1161 | 10.8206 | 0.0000 | 373.26 | 752.52 | 760.76 | 755.86 | 761.27 |
| EG | 0.1013 | – | 0.0682 | 373.95 | 751.90 | 757.39 | 754.13 | 757.65 |
| Lomax | 0.1161 | 10.8209 | – | 373.26 | 750.52 | 756.01 | 752.75 | 756.26 |
| Exp. | 0.1052 | – | – | 373.98 | 749.95 | 752.70 | 751.06 | 752.78 |

## 7. Conclusions

This paper introduced a logarithmic–gamma frailty (LGF) model for first-failure times with heavy-tailed risk. By combining a logarithmic mixing distribution for the latent number of competing failure causes with shared gamma frailty and exponential component lifetimes, the model yields a logarithmic mixture of Lomax distributions and nests several classical lifetime models, including the Lomax and exponential distributions, as boundary or limiting cases.

The proposed framework admits tractable series representations for the density, distribution, survival, and hazard functions and exhibits heavy-tailed survival behavior governed by the frailty parameter. Conditional on $N = n$, the model reduces to a Lomax distribution with a strictly decreasing

hazard rate. Because monotone hazard properties are not automatically preserved under mixing, we do not state a general monotonicity theorem for the marginal hazard; instead, representative marginal hazard shapes are illustrated numerically. Likelihood-based inference procedures were developed via direct maximization and an EM-type algorithm, and their behavior was examined through simulation and a real-data application. In first-failure-only settings, the mixing parameter $\eta$ can be weakly identifiable and may be estimated at the boundary (e.g., $\hat{\eta} = 0$), in which case the model appropriately reduces to its Lomax submodel.

*Sensitivity and extensions beyond exponential baselines*

We focused on exponential component lifetimes because the minimum-of-exponentials structure combined with gamma frailty yields tractable series expressions and a transparent Lomax-mixture interpretation. More generally, the same hierarchical first-failure construction can be formulated for alternative baseline families (e.g., Weibull or gamma) by specifying the conditional survival $S_{X|Z}(x \mid z)$ and using

$$S_{Y|N,Z}(y \mid n, z) = \{S_{X|Z}(y \mid z)\}^n,$$

followed by integrating over the frailty distribution and mixing over $N$. Although a full treatment of alternative baselines is beyond the scope of this paper, this representation makes clear how the framework extends beyond the exponential assumption and provides a basis for assessing sensitivity to baseline misspecification.

As a practical sensitivity check, one may conduct a misspecification experiment in which first-failure samples are generated under a Weibull baseline with shared gamma frailty and logarithmic system size, and then fit to the exponential-baseline LGF model to compare maximized log-likelihood values and hazard-shape behavior. This provides a direct assessment of robustness of inference for $(\theta,\ \lambda,\ \eta)$ under mild departures from exponentiality.

A practical limitation is that $\eta$ can be weakly identifiable from first-failure data alone, so boundary estimates (e.g., $\hat{\eta} = 0$) may occur, reducing the model to its Lomax submodel. Future research directions include extensions to interval-censored and right-censored data, regression formulations with covariates, and multivariate/shared frailty generalizations for dependent competing systems and multiple-failure or competing-risks settings.

## Use of Generative-AI tools declaration

The author declares that the use of AI tools is limited to language editing and checking the logical consistency of certain mathematical arguments. All scientific content, proofs, results, and conclusions were developed and independently verified by the author, who takes full responsibility for the work.

## Funding

This work was supported by the Deanship of Scientific Research, Vice Presidency for Graduate Studies and Scientific Research, King Faisal University, Saudi Arabia [Grant No. KFU261395].

## Conflict of interest

The author declares no conflicts of interest in this paper.

## References


1. J. Guo, X. Kong, N. Wu, L. Xie, Evaluating the lifetime distribution parameters and reliability of products using successive approximation method, *Qual. Reliab. Eng. Int.*, **40** (2024), 3280–3303. http://dx.doi.org/10.1002/qre.3559
2. M. Xu, H. Mao, q-weibull distributions: Perspectives and applications in reliability engineering, *IEEE T. Reliab.*, **74** (2025), 3112–3125. http://dx.doi.org/10.1109/tr.2024.3448289
3. Y. J. Yang, W. Wang, X. Y. Zhang, Y. L. Xiong, G. H. Wang, Lifetime data modelling and reliability analysis based on modified weibull extension distribution and bayesian approach, *J. Mech. Sci. Technol.*, **32** (2018), 5121–5126. http://dx.doi.org/10.1007/s12206-018-1009-8
4. M. E. Bakr, O. S. Balogun, A. A. El-Toony, A. M. Gadallah, Reliability analysis for unknown age class of lifetime distribution with real applications in medical science, *Symmetry*, **16** (2024), 2073–8994. http://dx.doi.org/10.3390/sym16111514
5. N. Feroze, U. Tahir, M. Noor-ul Amin, K. S. Nisar, M. S. Alqahtani, M. Abbas, et al., Applicability of modified weibull extension distribution in modeling censored medical datasets: A Bayesian perspective, *Sci. Rep.*, **12** (2022), 2045–2322. http://dx.doi.org/10.1038/s41598-022-21326-w
6. N. M. Alfaer, A. M. Gemeay, H. M. Aljohani, A. Z. Afify, The extended log-logistic distribution: Inference and actuarial applications, *Mathematics*, **9** (2021), 1386. http://dx.doi.org/10.3390/math9121386
7. S. Chowdhury, A. K. Nanda, A new lifetime distribution with applications in inventory and insurance, *Int. J. Qual. Reliab. Ma.*, **35** (2018), 527–544. http://dx.doi.org/10.1108/ijqrm-12-2016-0227
8. F. H. Riad, A. Radwan, E. M. Almetwally, M. Elgarhy, A new heavy tailed distribution with actuarial measures, *J. Radiat. Res. Appl. Sci.*, **16** (2023), 100562. http://dx.doi.org/10.1016/j.jrras.2023.100562
9. A. Hurwitz, O. S. Mitchell, Financial regret at older ages and longevity awareness, *J. Risk Insur.*, **92** (2025), 719–739. http://dx.doi.org/10.1111/jori.70008
10. R. C. Merton, Lifetime portfolio selection under uncertainty: The continuous-time case, *Rev. Econ. Stat.*, **51** (1969), 247. http://dx.doi.org/10.2307/1926560
11. K. K. Anakha, V. M. Chacko, On comparative lifetime analysis with the generalized Lindley distribution: Insights from joint adaptive progressive Type-II censoring, *J. Stat. Comput. Sim.*, **95** (2025), 2466–2493. http://dx.doi.org/10.1080/00949655.2025.2496397
12. J. Lei, W. Kuo, An order statistics perspective for system reliability, *Appl. Stoch. Model. Bus.*, **41** (2024). http://dx.doi.org/10.1002/asmb.2895
13. H. W. Jones, *Four problematic methods in reliability analysis*, In: 2025 Annual Reliability and Maintainability Symposium (RAMS), IEEE, 2025, 1–6. http://dx.doi.org/10.1109/rams48127.2025.10935161

14. J. Gillariose, M. M. Abdelwahab, J. Joseph, M. M. Hasaballah, A gauss hypergeometric-type model for heavy-tailed survival times in biomedical research, *Symmetry*, **17** (2025), 1795. http://dx.doi.org/10.3390/sym17111795

15. J. Yslas, Phase-type frailty models: A flexible approach to modeling unobserved heterogeneity in survival analysis, *Scand. Actuar. J.*, 2025, 1–29. http://dx.doi.org/10.1080/03461238.2025.2520586

16. M. Rahmouni, D. Ziedan, The weibull-generalized shifted geometric distribution: Properties, estimation, and applications, *AIMS Math.*, **10** (2025), 9773–9804. http://dx.doi.org/10.3934/math.2025448

17. M. Rahmouni, The doubly generalized exponential-geometric frailty distribution, *AIMS Math.*, **10** (2025), 30384–30428. http://dx.doi.org/10.3934/math.20251334

18. K. Adamidis, S. Loukas, A lifetime distribution with decreasing failure rate, *Stat. Probabil. Lett.*, **39** (1998), 35–42. http://dx.doi.org/10.1016/s0167-7152(98)00012-1

19. D. D. Hanagal, *Frailty models in public health*, Disease Modelling and Public Health, Part B, Handbook of Statistics, chapter Frailty Models in Public Health, Elsevier, **37** (2017), 209–247. http://dx.doi.org/10.1016/bs.host.2017.07.004

20. P. Hougaard, Frailty models for survival data, *Lifetime Data Anal.*, **1** (1995), 255–273. http://dx.doi.org/10.1007/bf00985760

21. C. D. Lai, M. Izadi, Generalized logistic frailty model, *Stat. Probabil. Lett.*, **82** (2012), 1969–1977. http://dx.doi.org/10.1016/j.spl.2012.06.012

22. T. A. Balan, H. Putter, A tutorial on frailty models, *Stat. Methods Med. Res.*, **29** (2020), 3424–3454. http://dx.doi.org/10.1177/0962280220921889

23. K. S. Lomax, Business failures: Another example of the analysis of failure data, *J. Am. Stat. Assoc.*, **49** (1954), 847–852. http://dx.doi.org/10.1080/01621459.1954.10501239

24. F. A. Moala, L. M. Garcia, A bayesian analysis for the parameters of the exponential-logarithmic distribution, *Qual. Eng.*, **25** (2013), 282–291. http://dx.doi.org/10.1080/08982112.2013.764431

25. M. Rahmouni, A. Orabi, A generalization of the exponential-logarithmic distribution for reliability and life data analysis, *Life Cycle Reliab. Safety Eng.*, **7** (2018), 159–171. http://dx.doi.org/10.1007/s41872-018-0049-5

26. A. S. Nayal, P. L. Ramos, A. Tyagi, B. Singh, Improving inference in exponential logarithmic distribution, *Commun. Stat.- Simul. C.*, 2025, 1–25. http://dx.doi.org/10.1080/03610918.2024.2446346

27. E. T. Lee, J. W. Wang, *Statistical methods for survival data analysis*, Wiley Series in Probability and Statistics, John Wiley & Sons, 2003. http://dx.doi.org/10.1002/0471458546

## Appendix: Robustness analysis

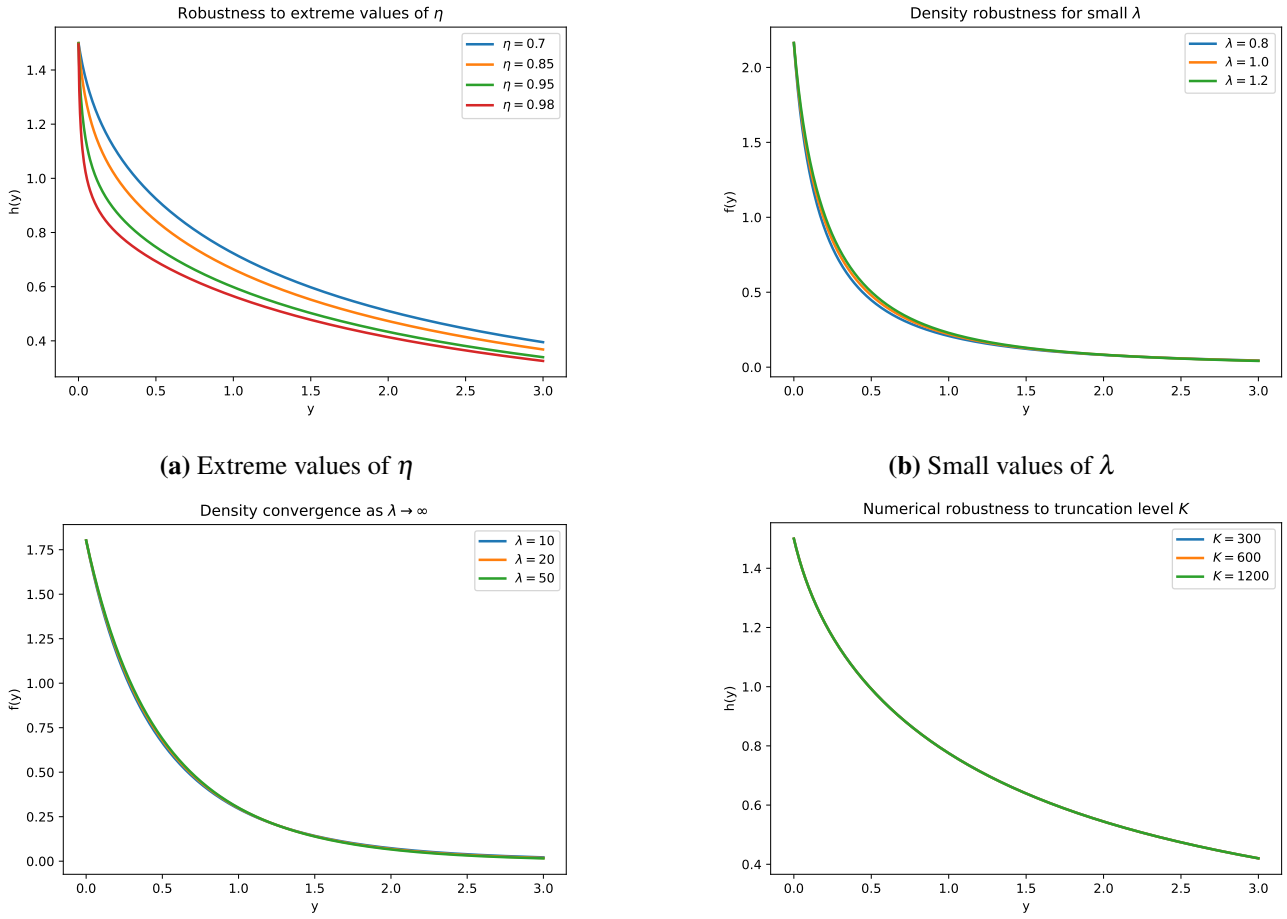


**(a)** Extreme values of $\eta$

**(b)** Small values of $\lambda$

**(c)** Large values of $\lambda$

**(d)** Truncation level $K$

**Figure 3.** Robustness analysis of the logarithmic–gamma frailty model for first-failure times. Panel (a) shows the marginal hazard for extreme values of the logarithmic parameter $\eta$; panel (b) shows density behavior for small values of the frailty parameter $\lambda$ (heavy-tailed regimes); panel (c) illustrates density behavior for large $\lambda$ (vanishing heterogeneity); panel (d) assesses numerical stability with respect to the series truncation level $K$ used to approximate the infinite sums.

Figure 3 provides numerical checks demonstrating that the LGF model is stable under extreme parameter configurations and under the truncation used to approximate the infinite series representations. Throughout, we focus on first-failure times, consistent with the model formulation in the main text.

**Extreme logarithmic mixing.** Figure 3(a) evaluates the marginal hazard when $\eta$ is close to its upper boundary, where the logarithmic mixing distribution places substantial mass on large latent system sizes. The resulting hazard curves remain smooth and well-behaved over the displayed range of $y$,

indicating no numerical pathologies in highly clustered settings.

**Heavy-tailed frailty regimes.** Figure 3(b) examines density stability for small values of $\lambda$, which correspond to strong unobserved heterogeneity and heavier tails. The density remains smooth across the considered values, showing that the numerical evaluation of the series is stable even in heavy-tailed regimes.

**Vanishing heterogeneity.** Figure 3(c) considers large $\lambda$, where the variance of the gamma frailty decreases, and the model approaches its exponential–logarithmic limiting behavior. The displayed density curves illustrate the continuity of the model as heterogeneity vanishes.

**Truncation robustness.** Figure 3(d) assesses sensitivity to the truncation level $K$ used in the infinite sums. The hazard curves for $K = 300$, 600, and 1200 are nearly indistinguishable, supporting that the numerical results reported in the paper are not artifacts of truncation and are stable for moderate values of $K$.

Overall, these checks support the numerical reliability of the proposed LGF model across a wide range of parameter values, including extreme clustering, heavy-tailed regimes, vanishing heterogeneity, and different truncation levels.


AIMS Press